

This is an electronic reprint of the original article. This reprint may differ from the original in pagination and typographic detail.

---

## Catalytic Role of Process Dust in SO<sub>2</sub>-to-SO<sub>3</sub> Conversion in Flash Smelting Heat Recovery Boilers

Lehmusto, Juho; Laurén, Tor; Lindgren, Mari

*Published in:*  
JOM Journal of the Minerals, Metals and Materials Society

*DOI:*  
[10.1007/s11837-019-03464-1](https://doi.org/10.1007/s11837-019-03464-1)

Published: 01/01/2019

*Document Version*  
Final published version

*Document License*  
CC BY

[Link to publication](#)

*Please cite the original version:*  
Lehmusto, J., Laurén, T., & Lindgren, M. (2019). Catalytic Role of Process Dust in SO<sub>2</sub>-to-SO<sub>3</sub> Conversion in Flash Smelting Heat Recovery Boilers. *JOM Journal of the Minerals, Metals and Materials Society*, 71(9), 3305–3313. <https://doi.org/10.1007/s11837-019-03464-1>

### General rights

Copyright and moral rights for the publications made accessible in the public portal are retained by the authors and/or other copyright owners and it is a condition of accessing publications that users recognise and abide by the legal requirements associated with these rights.

### Take down policy

If you believe that this document breaches copyright please contact us providing details, and we will remove access to the work immediately and investigate your claim.



TECHNICAL ARTICLE

# Catalytic Role of Process Dust in SO<sub>2</sub>-to-SO<sub>3</sub> Conversion in Flash Smelting Heat Recovery Boilers

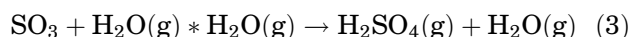
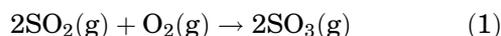
JUHO LEHMUSTO,<sup>1,3</sup> TOR LAURÉN,<sup>1</sup> and MARI LINDGREN<sup>2</sup>

1.—Laboratory of Inorganic Chemistry, Johan Gadolin Process Chemistry Centre, Abo Akademi University, Piispankatu 8, 20500 Turku, Finland. 2.—Outotec Research Center, Kuparitie 10, P.O. Box 69, 28101 Pori, Finland. 3.—e-mail: juho.lehmusto@abo.fi

The aim of this work is to examine the catalytic role of copper smelter, copper converter, and nickel smelter process dusts in SO<sub>2</sub>-to-SO<sub>3</sub> conversion at 750°C. To clarify the role of specific oxides in greater detail, synthetic dusts containing varying concentrations of either CuO or Fe<sub>3</sub>O<sub>4</sub> were also studied. All studied dusts catalyzed SO<sub>3</sub> conversion. Among the industrial flue dusts, the highest concentration of SO<sub>3</sub> formed in the presence of copper smelter dust. Comparing individual oxides, CuO had a greater impact on the SO<sub>3</sub> formation. Such catalytic effects of smelter dusts may lead to SO<sub>3</sub> concentrations in the process gas so high that sulfuric acid dew point corrosion may occur.

## INTRODUCTION

The flash smelting process is one of the most widely used methods to extract primary copper<sup>1</sup> and nickel<sup>2</sup> from sulfide ores using smelting and refining processes. The process is very cost-effective and environmentally sustainable because, once initiated, it is continuous and nearly autothermal.<sup>3</sup> Smelting of sulfide ores releases large quantities (20–70 vol.%) of sulfur dioxide (SO<sub>2</sub>) into the process gas, which is first cleaned then passed to a sulfuric acid plant for use as raw material.<sup>4</sup> Under suitable conditions, part of this SO<sub>2</sub> can be oxidized to sulfur trioxide (SO<sub>3</sub>) (Eq. 1), which can react further to sulfuric acid (H<sub>2</sub>SO<sub>4</sub>) due to the presence of humidity in the process gas, through a reaction involving either an adduct (Eq. 2)<sup>5,6</sup> or a water dimer (Eq. 3).<sup>7</sup>



Formation of H<sub>2</sub>SO<sub>4</sub> in the heat recovery boiler is undesirable for the following reasons: (1) it lowers the overall recovery of sulfur, (2) once formed, it is difficult to process into saleable products, and (3) it may cause corrosion of heat-transfer surfaces. Since the concentration of SO<sub>3</sub> in the process gas affects

the dew point temperature of sulfuric acid, the risk of corrosion becomes more pronounced in the later sections of the plant, where temperatures may be very close to the dew point of sulfuric acid. The cyclic temperature profile of equipment together with possible air leaks can further enhance damage originating from such sulfuric acid dew point corrosion.<sup>8</sup> Partly sintered process dust particles may adhere to heat-transfer surfaces in the heat recovery area, resulting in deposits that decrease the heat-transfer efficiency and block the gas flow path.<sup>9</sup> Such deposits can also act as initiation points for corrosion, if the temperature inside a deposit drops below the dew point temperature of H<sub>2</sub>SO<sub>4</sub>, enabling its condensation and resulting in corrosion and severe material degradation.<sup>10,11</sup> In fact, strong indications of such sulfuric acid-induced corrosion were observed in full-scale measurements carried out during operation of a copper flash smelter plant.<sup>11</sup>

In a previous study, the effect of the process gas temperature on the catalytic SO<sub>2</sub>-to-SO<sub>3</sub> conversion was addressed in the temperature range of 275–900°C,<sup>12</sup> revealing that the temperature and presence of process dust had a remarkable effect on the SO<sub>3</sub> formation. Among the tested temperatures, the concentration of formed SO<sub>3</sub> peaked at 750°C, which was thus chosen as the temperature in the current work. Thermodynamically, SO<sub>2</sub>-to-SO<sub>3</sub> conversion is reported to show a maximum at around 500°C in the absence of catalytic species.<sup>13</sup> However, the

presence of a suitable catalyst such as fly ash affects the kinetics and thermodynamics of Eq. 1, shifting this conversion maximum to about 700°C.

In addition to temperature, various other variables also affect the concentration of SO<sub>3</sub> formed, namely the partial pressures of SO<sub>2</sub> and O<sub>2</sub>, the presence and concentration of humidity, the content of alkaline, earth-alkaline, and catalytically active compounds in the process dust and deposits, the temperature–residence time profile of the plant, and the application of gas cleaning equipment.<sup>14–19</sup> Iron oxides, which are typically present in high concentrations (12–30 wt.%) in copper flash smelter dust,<sup>11,20,21</sup> have been reported to catalyze SO<sub>2</sub>-to-SO<sub>3</sub> conversion.<sup>14,16,17</sup> Other oxides that are present in large quantities in process dust include copper oxides such as CuO and Cu<sub>2</sub>O, silicon oxide (SiO<sub>2</sub>), and aluminum oxide (Al<sub>2</sub>O<sub>3</sub>).<sup>22,23</sup> Regarding SO<sub>2</sub>-to-SO<sub>3</sub> conversion, SiO<sub>2</sub> has been reported to be inert, whereas Al<sub>2</sub>O<sub>3</sub> catalyzes the conversion to some extent.<sup>14</sup> Although Cu<sub>2</sub>O has been reported to lower the activation energy of SO<sub>3</sub> according to Eq. 1,<sup>24</sup> very little information is available on the catalytic properties of copper oxides.

The aim of this work is to study how the chemical composition affects the catalytic properties of different flash smelter process dusts regarding the SO<sub>2</sub>-to-SO<sub>3</sub> conversion at 750°C. In addition, the catalytic effect of two oxides, viz. copper(II) oxide (CuO) and magnetite (Fe<sub>3</sub>O<sub>4</sub>), often found in process dust, was addressed. The results are expected to shed more light on the role of specific compounds in SO<sub>3</sub> formation. Better knowledge of factors affecting SO<sub>3</sub> formation in the heat recovery boiler is desired for process optimization and corrosion prevention.

## EXPERIMENTAL PROCEDURES

The catalytic properties of flue dusts were first studied using industrial flue dusts collected from a copper and a nickel smelting plant, then with synthetic process dusts consisting of either copper(II) oxide (CuO) or magnetite (Fe<sub>3</sub>O<sub>4</sub>). The industrial flue dust samples were collected from the heat recovery boilers of both copper and nickel plants, in addition to one dust sample collected from the converter of the copper plant. Prior to exposure of the synthetic dusts, two oxides, silica (SiO<sub>2</sub>; Merck, *pro analysi* grade) and alumina (Al<sub>2</sub>O<sub>3</sub>; Aldrich, 99%), were exposed under the same conditions as the samples. The goal was to identify an inert oxide to mix with the studied oxides to obtain different concentrations without changing the sample length. Based on the results (described in detail below), SiO<sub>2</sub> was chosen. The synthetic dusts contained 2 mol.%, 10 mol.%, or 25 mol.% of either CuO or Fe<sub>3</sub>O<sub>4</sub>, while the rest of the sample was inert SiO<sub>2</sub>. The effect of the type of iron oxide on the SO<sub>2</sub>-to-SO<sub>3</sub> conversion was studied preliminary, thus two parallel samples containing 10 mol.% hematite (Fe<sub>2</sub>O<sub>3</sub>) were exposed to the same conditions as the samples containing magnetite.

The experimental setup consisted of a narrow quartz glass reactor with inner diameter of around 8 mm, positioned inside a horizontal tube furnace. The sample and a KCl plug were inserted inside the quartz reactor. All samples were studied at temperature of 750°C, whereas the temperature of the KCl plug was kept at around 200°C to avoid condensation of possibly formed H<sub>2</sub>SO<sub>4</sub>. The temperatures were monitored using thermocouples positioned in the furnace but outside the reactor to avoid the possible participation of the thermocouples as catalysts in the studied SO<sub>2</sub>-to-SO<sub>3</sub> conversion. Due to the inertness of quartz in SO<sub>2</sub>-to-SO<sub>3</sub> conversion,<sup>14</sup> quartz wool was used to keep the deposit and KCl plug in place. The measurement principle is based on the ability of the KCl plug to capture SO<sub>3</sub> from the gas that is fed through it. This originates from the higher stability of K<sub>2</sub>SO<sub>4</sub> compared with KCl,<sup>25</sup> meaning that, if any SO<sub>3</sub> interacts with KCl, it will be converted to K<sub>2</sub>SO<sub>4</sub>. However, KCl is inert to SO<sub>2</sub> at 200°C, so the original process gas does not interact with the KCl plug. The measurement technique is described in greater detail in Ref. 12.

The density of the studied dusts varied greatly, so instead of having an equal mass, all samples had equal length of 6.0 cm. Due to the possible blockage of the reactor through dust sintering, a narrow gap was left above the sample. The mass of the KCl (Merck, suprapur 99.999%) plug was 0.5 g. The gas mixture mimicking genuine process gas consisted of 50 vol.% N<sub>2</sub>, 10 vol.% O<sub>2</sub>, and 40 vol.% SO<sub>2</sub>. In addition, one exposure for each industrial flue dust was also carried out in an SO<sub>2</sub>-free atmosphere. This was done to examine the possible SO<sub>3</sub> release from the deposit itself. In the exposures without SO<sub>2</sub>, the gas consisted of 90 vol.% N<sub>2</sub> and 10 vol.% O<sub>2</sub>. The sampling time was 5 min. During the heating, the reactor was flushed with a constant N<sub>2</sub> flow at the same rate as during the exposures, viz. 1 dm<sup>3</sup> min<sup>-1</sup> (RT). The exposures in the absence of SO<sub>2</sub> in the gas were carried out once, whereas all the other exposures were carried out twice.

A scanning electron microscope (LEO 1530 Gemini) coupled to an x-ray detector (Thermo Scientific UltraDry Silicon Drift Detector) and an energy-dispersive x-ray analysis system (Thermo Scientific ThermoNORAN Vantage x-ray) was used to estimate the particle size of the industrial flue dusts. In addition, the chemical composition of the dust samples was determined before and after the exposures using the same instrumentation. The microscope was operated under high vacuum (around 10<sup>-6</sup> mbar) at accelerating voltage of 20 kV in backscatter electron mode for imaging and EDX analysis.

To identify different sulfur-containing compounds in the process dusts, both solid and dissolved samples were analyzed to quantify the concentration of sulfur (Eltra CS 2000 induction furnace coupled with IR detectors) and SO<sub>4</sub><sup>2-</sup> (ion chromatograph, IC). In addition, a magnetite analyzer

(Satmagan 135) capable of quantifying magnetite concentrations in a nonmagnetic medium was used to distinguish hematite from magnetite in the industrial flue dusts.

X-ray powder diffraction (XRPD) was used to identify compounds in the dust samples. The XRPD measurements were performed using a Malvern Panalytical Empyrean x-ray diffractometer equipped with a Cu x-ray tube and PIXcel3D detector. Scans ( $2\theta$ ) were carried out between 10° and 100°. The diffractograms were matched using Malvern Panalytical HighScore Plus software and International Centre for Diffraction Data (ICDD) powder diffraction file (PDF)-4+ 2018.<sup>26</sup>

The KCl plug was dissolved in a known volume of deionized water, and the SO<sub>4</sub><sup>2-</sup> concentration was quantified using an ion chromatography system (IC, Metrohm Compact IC Pro with Metrosep anion Dual 2 column and Metrohm 732 IC detector) with 2 mM NaHCO<sub>2</sub> and 1.3 mM Na<sub>2</sub>CO<sub>3</sub> solutions as eluents. Due to the different retention times of Cl<sup>-</sup> and SO<sub>4</sub><sup>2-</sup> ions, they can be easily distinguished by ion chromatography.

## RESULTS AND DISCUSSION

In this study, industrial flue dusts collected from a copper and a nickel smelter plant were studied first to clarify their chemical composition and role in catalyzing the SO<sub>2</sub>-to-SO<sub>3</sub> conversion. Based on the results of XRPD analysis, SEM, and chemical analysis (Table I), CuO and Fe<sub>3</sub>O<sub>4</sub> were chosen to further specify the impact of these oxides on SO<sub>3</sub> formation in a simplified chemical environment provided by the synthetic dusts. Following the timeline of the work, the results for the industrial flue dusts are presented and discussed first in their own subsection, followed by another addressing the synthetic dusts.

### Industrial Flue Dusts

The morphology and particle size of the dusts did not change significantly during the exposure (Figs. 1 and 2). The dust samples exposed in the absence of SO<sub>2</sub> were also imaged, but no differences in the morphology of the dust particles were

observed. All samples contained spherical particles, indicating that the particles were partly molten at some point of the process line.<sup>27</sup> If the particles reach heat-transfer surfaces while in the partly molten state, they might adhere to the surfaces, resulting in deposits that decrease the heat-transfer efficiency and block the gas flow path.<sup>9</sup> Based on EDX spot analyses, the spherical particles consisted mainly of Cu, S, and O, most likely as anhydrous copper sulfate (CuSO<sub>4</sub>).<sup>28</sup> In addition to CuSO<sub>4</sub>, the round-shaped particles contained small concentrations of Fe, Pb, and Zn. The analyzed dust samples contained altogether more than 15 different elements, the most abundant of which are listed in Table II as averages of three EDX analyses. The copper smelter process dust consisted mainly of Cu, Fe, O, and S, the copper smelter converter dust contained mostly Cu, O, Pb, and S, while the nickel smelter process dust contained Fe, Ni, and O. The presence of lead most likely originated from condensation lead vaporized earlier in the process line. Other metals with low melting points that can be found in converter dust in larger quantities are zinc and arsenic.<sup>22</sup> Although As, Zn, and Pb have not been reported to catalyze SO<sub>2</sub>-to-SO<sub>3</sub> conversion, they may play a crucial role in deposit formation due to the low melting points of their compounds such as As<sub>2</sub>O<sub>3</sub>, ZnCl<sub>2</sub>, and PbCl<sub>2</sub>, to name a few. The sulfur content of the nickel smelter process dust was clearly lower than those measured for the copper smelter dusts. The sulfur contents of the reference samples were significantly lower than in the samples exposed in the presence of SO<sub>2</sub>, indicating that especially copper smelter dust released sulfur-containing species at high temperatures. Based on XRD analyses, the following species were identified with high certainty: Cu<sub>2</sub>SO<sub>4</sub>, CuO, and PbSO<sub>4</sub> in converter dust, Cu<sub>2</sub>SO<sub>4</sub>, Fe<sub>3</sub>O<sub>4</sub>, Fe<sub>2</sub>O<sub>3</sub>, and SiO<sub>2</sub> in copper smelter dust, and Ni<sub>0.6</sub>Fe<sub>2.4</sub>O<sub>4</sub> in nickel smelter dust. It should be borne in mind that, considering the actual complexity of the dusts, their compositions are far more diverse than listed here. However, identification of tracer species in process dusts lies beyond the scope of this work.

Putting the focus on iron and copper, both were found at concentrations of at least 10 wt.% in copper smelter dust, whereas the converter dust was rich in copper and the nickel smelter dust in iron (Table II). Based on EDX results, the concentration of iron and copper oxides cannot be reliably quantified, but the analyzed SO<sub>4</sub><sup>2-</sup> concentrations (Table I) indicated that roughly 30% of the sulfur in the copper smelter dust was present as sulfates, whereas 4% and 8% of the sulfur was bound in sulfates in the nickel smelter and converter dust, respectively. Regarding iron oxides, roughly 21%, 41%, and 1% of the iron were in the form of magnetite in the copper smelter, nickel smelter, and converter dust, respectively. Other compounds containing Fe, Cu, and/or O included, for example, CuS, FeS, PbSO<sub>4</sub>, and As<sub>2</sub>O<sub>5</sub>.<sup>20,22,29</sup> Based on these

**Table I. Concentrations of total sulfur, sulfates, and magnetite in the studied process dusts**

Sample	S <sub>tot</sub> (wt.%)	SO <sub>4</sub> <sup>2-</sup> (%)	Fe <sub>3</sub> O <sub>4</sub> (%)
Cu dust	9.7	28.8	20.9
Ni dust	1.4	4.1	41.1
Conv. dust	10.5	7.9	0.9

The analyses were carried out with an ion chromatograph, a magnetite analyzer, and an induction furnace coupled with IR detectors.

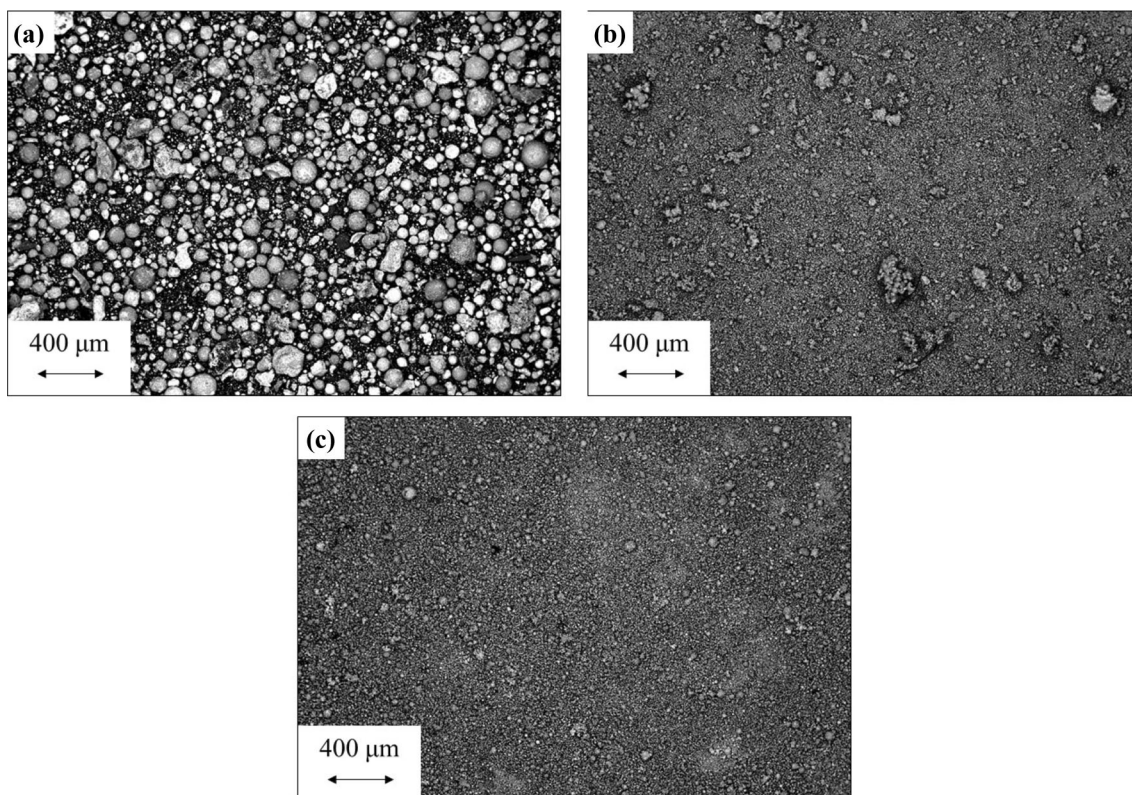


Fig. 1. Industrial flue dusts before exposure: copper smelter converter dust (a), copper smelter process dust (b), and nickel smelter process dust (c).

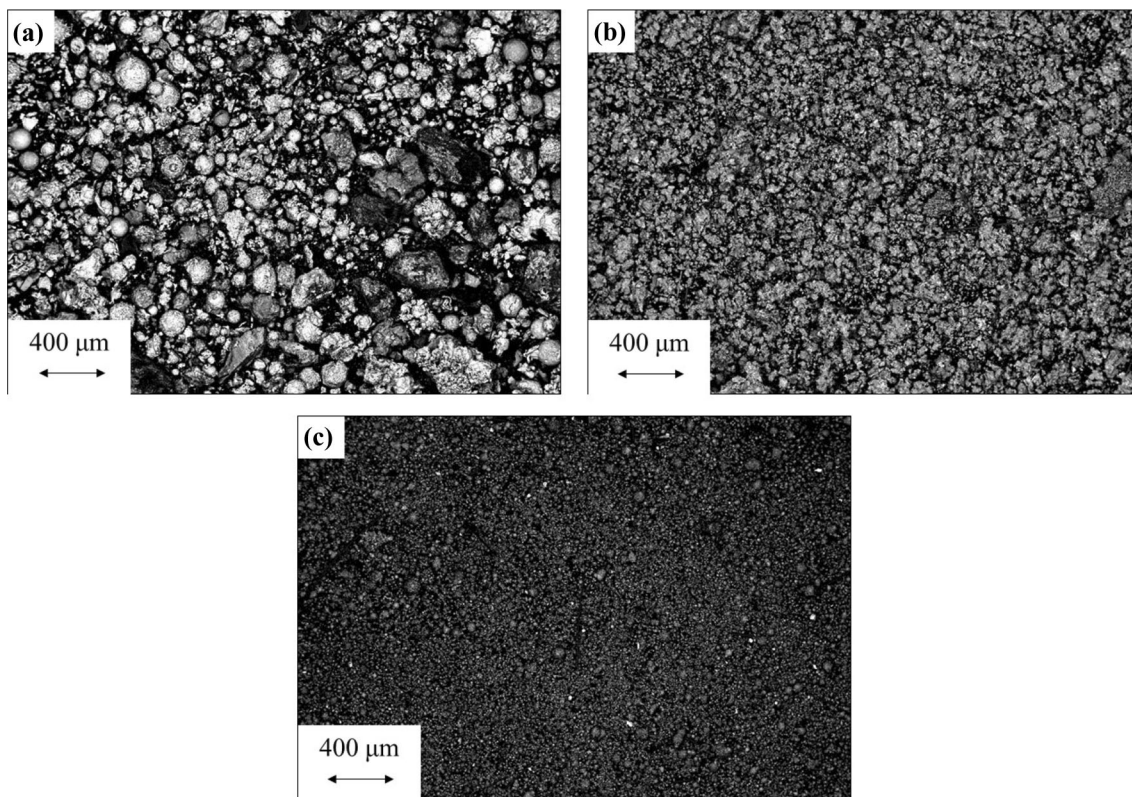


Fig. 2. Industrial flue dusts after exposure at 750°C: copper smelter converter dust (a), copper smelter process dust (b), and nickel smelter process dust (c).

**Table II. Concentrations of main elements in studied process dusts, analyzed with SEM-EDS; values presented in weight percentages**

Element	Cu dust as received	Cu dust exposed	Cu dust reference	Conv. dust as received	Conv. dust exposed	Conv. dust reference	Ni dust as received	Ni dust exposed	Ni dust reference
As	3.7	3.1	4.7	3.1	0.9	1.1	3.4	–	–
Cu	23.8	24.5	26.3	27.3	55.8	49.4	3.1	2.5	3.0
Fe	11.4	11.6	24.0	1.1	1.7	1.8	35.2	37.6	41.2
Ni	–	–	–	–	1.0	0.6	12.1	12.7	13.6
O	38.5	37.6	26.8	37.1	21.8	24.0	32.4	32.5	29.3
Pb	–	–	–	9.7	3.4	4.3	–	–	–
S	14.8	13.2	1.4	11.6	4.2	1.1	4.9	3.1	2.3
Si	1.7	3.6	6.7	1.2	6.5	11.3	3.7	6.4	4.7
Zn	3.9	4.1	5.7	4.4	2.2	3.2	0.2	0.1	0.2

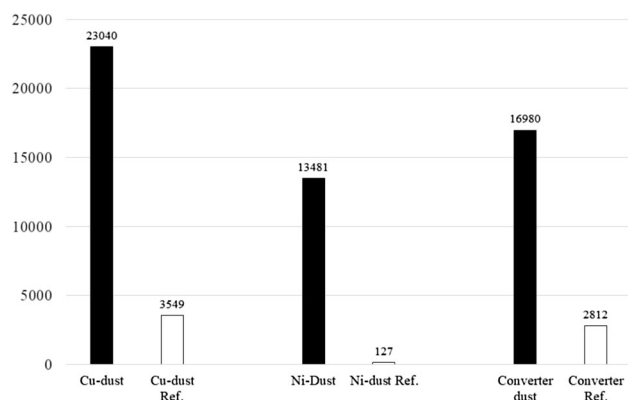


Fig. 3. Concentrations of SO<sub>3</sub> formed at 750°C in the reaction catalyzed by industrial flue dusts. The reference samples were exposed without SO<sub>2</sub> in the atmosphere.

analyses and previous results,<sup>14,16,17,24</sup> iron and copper oxides can be considered responsible for the catalyzed SO<sub>3</sub> formation in the present study. With copper content of roughly 24 wt.% and iron content of 11 wt.%, the copper smelter dust catalyzed SO<sub>3</sub> formation the most, compared with copper converter dust (27 wt.% Cu) or nickel smelter dust (35 wt.% iron). This suggests that the presence of copper as an oxide has a greater impact on the catalyzed SO<sub>3</sub> formation than iron oxide. The role of the two oxides is addressed in detail below when synthetic dusts are discussed.

All studied dusts catalyzed SO<sub>3</sub> formation, with 23,000 ppm, 13,500 ppm, and 17,000 ppm SO<sub>3</sub> formed in the presence of copper smelter dust, nickel smelter dust, and copper converter dust, respectively (Fig. 3). Since the concentration of SO<sub>2</sub> in the synthetic process gas was 40% (400,000 ppm), the concentrations of SO<sub>2</sub> converted to SO<sub>3</sub> according to Eq. 1 were 5.8%, 3.4%, and 4.3% in the presence of copper smelter dust, nickel smelter dust, and copper converter dust, respectively. The

concentrations of formed SO<sub>3</sub> are somewhat higher compared with the 1–3% reported previously in the same temperature range,<sup>30</sup> but the concentration of formed SO<sub>3</sub> depends, among other factors, on the SO<sub>2</sub> concentration of the process gas, which can vary greatly depending on the feed, copper production method, and location inside the copper processing line. Despite the fact that the nickel smelter process dust clearly catalyzed SO<sub>2</sub>-to-SO<sub>3</sub> conversion, according to industry, less corrosion-related problems are detected in nickel flash smelters compared with copper flash smelters. The reason for this remains ambiguous, but differences in process conditions or feed impurities, or a lower deposit build-up rate, may play a role.

In the case of copper smelter dust, there was also notable SO<sub>3</sub> formation in the absence of SO<sub>2</sub> in the process gas. Since the deposits exposed in the absence of SO<sub>2</sub> contained very little sulfur after the exposures (< 1.5 wt.%), the formed SO<sub>3</sub> most likely stems from temperature-induced decomposition/oxidation of sulfur-containing species such as sulfates and/or sulfides within the deposit. It is worth mentioning that, from a measurement/technical point of view, the results are very close to those reported previously,<sup>12</sup> indicating good reproducibility of the method.

### Synthetic Process Dusts

To select an inert filler oxide for the synthetic dusts, pure SiO<sub>2</sub> and Al<sub>2</sub>O<sub>3</sub> were exposed to the gas mixture at 750°C for 5 min to confirm that the filler oxide would not contribute to SO<sub>3</sub> formation. The concentrations of formed SO<sub>3</sub> in the presence of SiO<sub>2</sub> and Al<sub>2</sub>O<sub>3</sub> were 120 ppm and 80 ppm, respectively. Part of the formed SO<sub>3</sub> originates from homogeneous (thermal) conversion, induced by the temperature (Eqs. 1 and 4)<sup>31–33</sup> and enhanced by humidity (Eqs. 5 and 6).<sup>33</sup> At 750°C, roughly 25 ppm SO<sub>3</sub> was formed from the gas containing 40 vol.% through homogeneous conversion in

10 min, indicating a minor effect of homogeneous conversion on the overall concentration of formed  $\text{SO}_3$ .<sup>12</sup> When the effect of homogeneous conversion is taken into account, either of the tested inert oxides could be used as a filler oxide in the synthetic dusts, because the concentrations of formed  $\text{SO}_3$  were expected to be so much higher than the share originating from the inert oxide, and homogeneous conversion can be neglected.  $\text{SiO}_2$  was selected due to its better handleability.  $\text{Al}_2\text{O}_3$  has been previously reported to slightly enhance  $\text{SO}_3$  formation,<sup>14</sup> although this could not be observed in the present study. The exact reason for this difference can only be speculated upon, but the concentrations of oxygen (10 vol.% in this study versus 60 vol.% in Ref. 14) and/or  $\text{SO}_2$  (40 vol.% in this study versus 1000 ppm in Ref. 14) in the gas mixture might explain the divergence in the results.



Based on the XRD results of the industrial flue dusts and previous calculations,<sup>34</sup> copper has two stable oxides at temperatures relevant to a flash smelter heat recovery boiler, viz. cuprous oxide ( $\text{Cu}_2\text{O}$ ) and cupric oxide ( $\text{CuO}$ ). Cupric oxide is the stable form at temperatures below 900°C and was therefore selected for the exposures with synthetic dusts.  $\text{Fe}_3\text{O}_4$  was selected on the basis of the chemical analyses (Table I) and previous findings.<sup>20,22</sup>

Both studied oxides ( $\text{CuO}$  and  $\text{Fe}_3\text{O}_4$ ) catalyzed  $\text{SO}_2$ -to- $\text{SO}_3$  conversion, although the impact of  $\text{CuO}$  was remarkably greater (Fig. 4). Due to the lower molar mass of  $\text{CuO}$  compared with  $\text{Fe}_3\text{O}_4$ , the

concentration of  $\text{CuO}$  in grams is smaller than the concentration of  $\text{Fe}_3\text{O}_4$  for the same molar fraction. This suggests that  $\text{CuO}$  is a more efficient catalyst than  $\text{Fe}_3\text{O}_4$  in  $\text{SO}_2$ -to- $\text{SO}_3$  conversion. This trend can partly be seen in the results for the industrial flue dusts, as the copper smelter dust with high copper concentration formed more  $\text{SO}_3$  than the nickel smelter dust with high iron concentration. The higher  $\text{SO}_3$  concentration formed by the copper smelter dust than by the copper converter dust can be explained by the presence of both iron and copper in the smelter dust.

The concentration of oxides did not have an unequivocal effect on the concentration of formed  $\text{SO}_3$ ; comparing the samples with 2 mol.% and 10 mol.% of either oxide, the  $\text{SO}_3$  concentration increased. However, a decrease was observed when comparing the samples with 10 mol.% and 25 mol.% of either oxide. The concentration of formed  $\text{SO}_3$  has been reported to increase linearly as a function of  $\text{Fe}_2\text{O}_3$  at 700°C up to 25 wt.% of  $\text{Fe}_2\text{O}_3$ ,<sup>17</sup> but similar behavior was not observed in this work. The reason was not investigated further, but it should be noted that the experimental setups and methods used to quantify the formed  $\text{SO}_3$  were completely different. Interestingly, the catalyst concentration has also been reported to show a maximum, above which higher catalyst concentrations result in a lower conversion rate.<sup>35</sup> The similar results of the exposures with 10 mol.%  $\text{Fe}_3\text{O}_4$  or  $\text{Fe}_2\text{O}_3$  suggest that  $\text{Fe}_3\text{O}_4$  oxidized to  $\text{Fe}_2\text{O}_3$ , which occurs at temperatures above 500°C<sup>36</sup> at oxygen partial pressures well below that in the present study.<sup>37</sup> Formation of  $\text{Fe}_2\text{O}_3$  was verified by XRD analysis after the exposure, but the point of the exposure at which this transition takes place remains unclear. Therefore, it is better to consider the results in the light of iron oxides in general rather than focusing on a specific type of iron oxide. Since both iron and

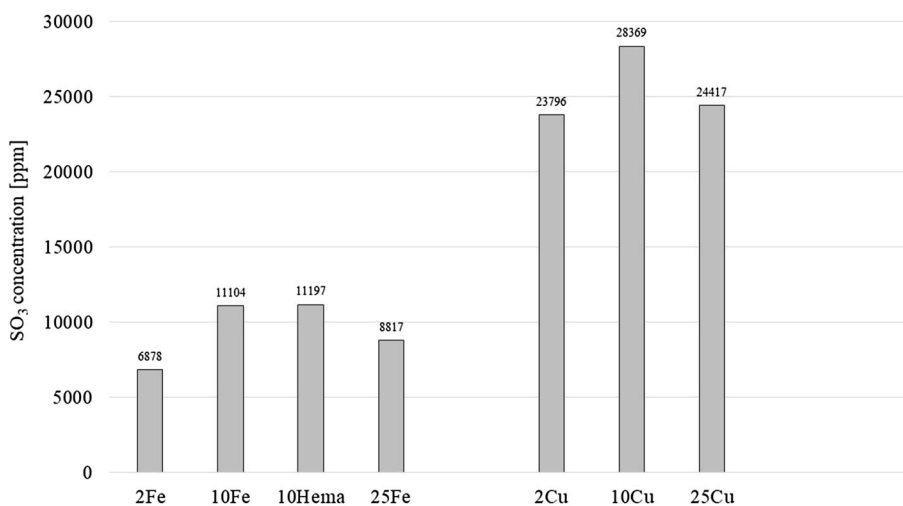


Fig. 4. Concentrations of  $\text{SO}_3$  formed at 750°C as a function of  $\text{Fe}_3\text{O}_4$  content (left-hand set) or  $\text{CuO}$  content (right-hand set). In the sample "Hema10,"  $\text{Fe}_2\text{O}_3$  was used instead of  $\text{Fe}_3\text{O}_4$ .

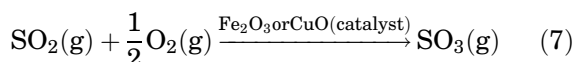
copper are present in the process dust and in deposits of the heat recovery boiler of a smelter, it is a justifiable assumption that both oxides are responsible for SO<sub>3</sub> formation in the heat recovery boiler of a smelter plant.

new computational approaches based on an artificial neural network model<sup>42</sup> or Vandermonde matrix<sup>43</sup> have been developed to estimate and predict the effect of the SO<sub>3</sub> concentration on the sulfuric acid dew point temperature. However, none

$$T_{\text{dewpoint}} = \frac{1000}{\{2.276 - 0.02943 \times \ln(p_{\text{H}_2\text{O}}) - 0.0858 \times \ln(p_{\text{SO}_3}) + 0.0062 \times \ln(p_{\text{H}_2\text{O}}) \times \ln(p_{\text{SO}_3})\}} \quad (8)$$

### Relationship Between SO<sub>3</sub> and Sulfuric Acid Dew Point

Based on these results, it is clear that both the industrial and synthetic deposits catalyzed and enhanced SO<sub>3</sub> formation. In addition to Fe<sub>2</sub>O<sub>3</sub> and CuO, other oxides such as PbO are also known to catalyze SO<sub>2</sub>-to-SO<sub>3</sub> conversion.<sup>30</sup> Although more research should be carried out for comprehensive clarification of which oxides in smelter plant deposits are relevant for SO<sub>2</sub>-to-SO<sub>3</sub> conversion, iron and copper oxide contribute significantly to SO<sub>3</sub> formation (Eq. 7). In addition to a suitable catalyst, formation of SO<sub>3</sub> in the heat recovery boiler requires oxygen, which is available due to its addition to the process to ensure effective sulfation of the flue dust. It should also be noted that, in addition to SO<sub>3</sub> formation in the heat recovery boiler, SO<sub>3</sub> can also form in the smelting or converting furnace and when entering the heat recovery boiler, increasing the overall concentration of SO<sub>3</sub>.



As mentioned in the "Introduction," the formation of SO<sub>3</sub> together with the presence of humidity enables sulfuric acid (H<sub>2</sub>SO<sub>4</sub>) formation. The dew point temperature of H<sub>2</sub>SO<sub>4</sub> depends on the SO<sub>3</sub> and H<sub>2</sub>O concentrations.<sup>31</sup> Different empirical equations have been proposed to predict the dew point of sulfuric acid as a function of the concentrations of SO<sub>3</sub> and H<sub>2</sub>O. The Verhoff-Banchero equation (Eq. 8)<sup>38</sup> has been successfully used in applications addressing lower SO<sub>3</sub> concentrations,<sup>31,39,40</sup> but is not accurate when applied to acid dew point calculations with very low SO<sub>3</sub> and high H<sub>2</sub>O concentrations.<sup>41</sup> The partial pressures in Eq. 8 are expressed in mmHg, and the sulfuric acid dew point in K. Another equation (Eq. 9)<sup>9</sup> provides better predictions of the acid dew point at high H<sub>2</sub>O concentrations but loses accuracy at low H<sub>2</sub>O concentrations.<sup>41</sup> The partial pressures in Eq. 9 are expressed in mmHg, and the sulfuric acid dew point in K. To overcome the shortcomings of these two equations, a more recent equation (Eq. 10), based on 188 validated data points, has been developed.<sup>41</sup> The partial pressures in Eq. 9 are expressed in mmHg, and the sulfuric acid dew point in °C. In addition to the equations presented above,

of the abovementioned approaches has been developed to predict the sulfuric acid dew point for SO<sub>3</sub> concentrations above 1000 ppm. Therefore, before these models can be applied to flash smelting environments, work should be carried out to validate the existing models for high SO<sub>3</sub> concentrations. Another possibility is to develop a new model which takes high SO<sub>3</sub> concentrations into account.

$$T_{\text{dewpoint}} = 365.6905 + 11.9864 \ln p_{\text{H}_2\text{O}} + 4.70336 \ln p_{\text{SO}_3} + (0.446 \ln p_{\text{SO}_3} + 5.2572)^{2.19} \quad (9)$$

$$T_{\text{dewpoint}} = 150 + 11.664 \ln p_{\text{SO}_3} + 8.13281 \ln p_{\text{H}_2\text{O}} - 0.383226 \ln p_{\text{SO}_3} \times \ln p_{\text{H}_2\text{O}} \quad (10)$$

To provide a perspective on how the measured SO<sub>3</sub> concentrations might affect the sulfuric acid dew point, it was calculated using all three equations presented above. The results are presented in Table III. The calculations were carried out for a humidity level of 5 vol.% (38 mmHg), a typical value for copper flash smelter heat recovery boilers. Depending on the equation used, the calculated dew point temperatures differ by 30 K at most, with Eq. 8 predicting the highest dew point temperatures, Eq. 9 the lowest values, and Eq. 10 intermediate values. As mentioned above, none of these equations has been validated for high SO<sub>3</sub> concentrations, so it cannot be stated which one would be most suitable for application in the flash smelter environment. Nevertheless, the large deviation in dew point temperatures obtained when using the different equations suggests that a predictive tool applicable for high SO<sub>3</sub> concentrations is required. Among the calculated dew point temperatures, the highest sulfuric acid dew point of 233°C is only around 40°C below the lowest heat-transfer surface temperature of 275°C. Although the calculated value is most likely an overestimation, it demonstrates how close to one another the material surface temperature and sulfuric acid dew point temperatures might be. This becomes even more important in situations in which the heat-transfer surface temperature might decrease below the

**Table III. Sulfuric acid dew points ( $T_{\text{dew}}$ ) calculated using Eqs. 8–10**

Sample	SO <sub>3</sub> (ppm)	$p(\text{SO}_3)$ (mmHg)	$T_{\text{dew}}$ (K) Eq. 8	$T_{\text{dew}}$ (K) Eq. 9	$T_{\text{dew}}$ (K) Eq. 10	$T_{\text{dew}}$ (°C) Eq. 8	$T_{\text{dew}}$ (°C) Eq. 9	$T_{\text{dew}}$ (°C) Eq. 10
Copper smelter	23,040	17.5104	503	468	482	230	195	209
Copper converter	16,980	12.9048	498	466	479	225	193	206
Nickel smelter	13,481	10.24556	495	464	477	221	191	203
2 mol.% Fe <sub>3</sub> O <sub>4</sub>	6878	5.22728	484	459	470	211	185	197
10 mol.% Fe <sub>3</sub> O <sub>4</sub>	11,104	8.43904	492	463	475	218	190	201
10 mol.% Fe <sub>2</sub> O <sub>3</sub>	11,197	8.50972	492	463	475	219	190	202
25 mol.% Fe <sub>3</sub> O <sub>4</sub>	8817	6.70092	488	461	472	215	188	199
2 mol.% CuO	23,796	18.08496	504	469	482	230	196	209
10 mol.% CuO	28,369	21.56044	506	470	484	233	197	211
25 mol.% CuO	24,417	18.55692	504	469	483	231	196	210

sulfuric acid dew point due to pressure fluctuations or maintenance shutdowns, resulting in sulfuric acid condensation and, most likely, material degradation. It should be noted that the calculations presented in Table III were carried out at only one humidity level. Since the sulfuric acid dew point temperature depends also on the partial pressure of H<sub>2</sub>O in the process gas, factors such as air leakage could increase the concentration of water in the process gas and thereby affect the acid dew point temperature. Despite the uncertainty regarding the accuracy of the calculated dew point temperature, it is obvious that smelter dusts play a role in SO<sub>3</sub> formation. It has been reported that, at temperatures above 400°C, SO<sub>2</sub> is the favored species of oxidized sulfur instead of SO<sub>3</sub>.<sup>9</sup> However, the high concentration of SO<sub>2</sub> in the smelter process gas and the presence of a suitable catalyst enable formation of SO<sub>3</sub> in quantities high enough to lower the sulfuric acid dew point temperature in a flash smelter.

### CONCLUSION

The aim of this work is to examine the catalytic role of both genuine flash smelter flue dusts and synthetic dusts in SO<sub>2</sub>-to-SO<sub>3</sub> conversion at 750°C by exposing copper smelter dust, copper converter dust, nickel smelter dust, and synthetic dusts with different CuO or Fe<sub>3</sub>O<sub>4</sub> content to synthetic process gas with 40 vol.% SO<sub>2</sub>. After exposure, the concentration of formed SO<sub>3</sub> was quantified. The main conclusions can be summarized as follows:

- All the industrial flue dusts catalyzed SO<sub>2</sub>-to-SO<sub>3</sub> conversion: copper smelter dust the most and nickel smelter dust the least.
- Regarding the synthetic deposits, both studied oxides (CuO and Fe<sub>3</sub>O<sub>4</sub>) catalyzed formation of SO<sub>3</sub>.
- Among the two studied oxides, CuO had a greater influence on the SO<sub>3</sub> formation than Fe<sub>3</sub>O<sub>4</sub>.
- The greater conversion efficiency of CuO explains the higher concentrations of SO<sub>3</sub> formed in the presence of industrial flue dusts with high copper content.
- The concentration of catalytic oxide in the synthetic dusts did not play a major role in terms of the conversion efficiency.
- The catalytic abilities of the dusts might form concentrations of SO<sub>3</sub> sufficient to enable sulfuric acid dew point corrosion at temperatures close to the surface temperatures of heat-transfer components in flash smelter heat recovery boilers.

### ACKNOWLEDGEMENTS

Open access funding provided by Abo Akademi University (ABO). This work was carried out within the Academy of Finland Project “Novel Approaches to Study Corrosion Mechanisms in High-temperature Industrial Processes” (Decision No. 296435). Financial support from Boliden Harjavalta and Outotec is gratefully acknowledged. In addition, the authors would like to thank Mr. Janne Hautamäki

for the dust samples, Mr. Luís Bezerra for carrying out the IC analyses, and Mr. Linus Silvander for operating the SEM apparatus.

### OPEN ACCESS

This article is distributed under the terms of the Creative Commons Attribution 4.0 International License (<http://creativecommons.org/licenses/by/4.0/>), which permits unrestricted use, distribution, and reproduction in any medium, provided you give appropriate credit to the original author(s) and the source, provide a link to the Creative Commons license, and indicate if changes were made.

### REFERENCES

1. I.V. Kojo, A. Jokilaakso, and P. Hanniala, *JOM* 52, 57 (2000).
2. T. Mäkinen and P. Taskinen, *Trans. Inst. Min. Metall. Sect. C* 117, 86 (2008).
3. M.E. Schelsinger, M.J. King, K.C. Sole, and W.G. Davenport, *Extractive Metallurgy of Copper*, 5th ed. (Amsterdam: Elsevier, 2011), pp. 89–110.
4. T. Ranki-Kilpinen, E.J. Peuraniemi, M., and Mäkinen, in *Sulfide Smelting 2002* (TMS, Warrendale, 2002), pp. 261–272.
5. E.R. Lovejoy, D.R. Hanson, and L.G. Huey, *J. Phys. Chem.* 100, 19911 (1996).
6. K. Morokuma and C. Muguruma, *J. Am. Chem. Soc.* 116, 10316 (1994).
7. J.T. Jayne, U. Poeschl, Y. Chen, D. Dai, L. Molina, D.R. Worsnop, C.E. Kolb, and M.J. Molina, *J. Phys. Chem. A* 101, 10000 (1997).
8. R. Ebara, F. Tanaka, and M. Kawasaki, *Eng. Fail. Anal.* 33, 29 (2013).
9. A.G. Okkes, *Hydrocarb. Process.* 66, 53 (1987).
10. J.M. Blanco and F. Pena, *Appl. Therm. Eng.* 28, 777 (2008).
11. J. Lehmusto, D. Stenlund, M. Lindgren, and P. Yrjas, *Oxid. Met.* 87, 199 (2017).
12. J. Lehmusto, E. Vainio, T. Laurén, and M. Lindgren, *Metall. Mater. Trans. B* 49, 434 (2018).
13. L.P. Belo, L.K. Elliott, R.J. Stanger, R. Spörl, K.V. Shah, J. Maier, and T.F. Wall, *Energy Fuels* 28, 7243 (2014).
14. T.L. Jørgensen, H. Linbjerg, and P. Glarborg, *Chem. Eng. Sci.* 62, 4496 (2007).
15. D. Fleig, K. Andersson, and F. Johnsson, *Ind. Eng. Chem. Res.* 51, 9483 (2012).
16. P.M. Foster, *Atmos. Environ.* 3, 157 (1969).
17. P. Marier and H.P. Dibbs, *Thermochim. Acta* 8, 155 (1974).
18. R. Spörl, J. Walker, L. Belo, K. Shah, R. Stanger, J. Maier, T. Wall, and G. Scheffknecht, *Energy Fuels* 28, 5296 (2014).
19. D. Fleig, M.U. Alzueta, F. Normann, M. Abián, K. Andersson, and F. Johnsson, *Combust. Flame* 160, 1142 (2013).
20. T. Markova, B. Boyanov, S. Pironkov, and N. Shopov, *J. Min. Metall. Sect. B* 36, 195 (2000).
21. R.K. Jana, B. Gorai, and Premchand, *Environmental and Waste Management* (NML: Jamshedpur, 1998), pp. 167–173.
22. C. Samuelsson and G. Carlsson, *CIM Bull.* 94, 111 (2001).
23. D.O. Okanigbe, A.P.I. Popoola, and A.A. Adeleke, *Procedia Manuf.* 7, 121 (2017).
24. G.M. Schwab and E. Kaldis, *Naturwissenschaften* 50, 516 (1963).
25. A. Pettersson, L.-E. Åmand, and B.-M. Steenari, *Fuel* 88, 1758 (2009).
26. ICDD, *PDF-4+ 2018 (Database)*, in ed. by S. Kabekkodu (International Centre for Diffraction Data, Newtown Square, 2018).
27. U. Kleinhans, C. Wieland, F.J. Frandsen, and H. Spliethoff, *Prog. Energy Combust. Sci.* 68, 65 (2018).
28. A. Morales, M. Cruells, A. Roca and R. Bergo, *Characterization of flue dusts from a copper smelter furnace, copper recovery and arsenic stabilization*, in ed. by P.A. Riveros, D.G. Dixon, D.B. Dreisinger, and M.J. Collins *The John E. Dutrizac International Symposium on Copper Hydrometallurgy, Cu 2007, Volume IV* (Canadian Institute of Mining, Metallurgy and Petroleum, Toronto, 2008), pp. 177–189.
29. T. Kurosawa, T. Yagishi, K. Togo, and T. Kato, *J-STAGE* 89, 107 (1973).
30. S. Sarkar, *JOM* 34, 43 (1982).
31. E. Vainio, T. Laurén, N. DeMartini, A. Brink, and M. Hupa, *J. For.* 4, 14 (2014).
32. R.J.S. Eloi, C.J. Newman, and G. Macfarlane, *CIM Bull.* 87, 77 (1994).
33. V. Montenegro, H. Sano, and T. Fujisawa, *Miner. Eng.* 49, 184 (2013).
34. T. Ranki-Kilpinen, *Sulphation of Cuprous and Cupric Oxide Dusts and Heterogeneous Copper Matte Particles in Simulated Flash Smelting Heat Recovery Boiler Conditions*, Doctoral Thesis (Helsinki University of Technology, 2004).
35. M.-C. Kim, *Appl. Chem. Eng.* 23, 588 (2012).
36. K.F. McCarty, M. Monti, S. Nie, D.A. Siegel, E. Starodub, F. El Gabaly, A.H. McDaniel, A. Shavorskiy, T. Tylyszczak, H. Bluhm, N.C. Bartelt, and J. de la Figuera, *J. Phys. Chem. C* 118, 19768 (2014).
37. H. Sakai, T. Tsui, and K. Naito, *J. Nucl. Sci. Technol.* 21, 844 (1984).
38. F. Verhoff and J. Banchemo, *Chem. Eng. Proc.* 70, 71 (1974).
39. W.M.M. Huijbregts and R.G.I. Leferink, *Anti-Corros. Methods M* 51, 173 (2004).
40. V. Ganapathy, *Hydrocarb. Process.* 68, 57 (1989).
41. B. ZareNezhad, *Oil Gas J.* 107, 60 (2009).
42. B. ZareNezhad and A. Aminiam, *Energ. Convers. Manag.* 52, 911 (2011).
43. A. Bahadori, *Appl. Therm. Eng.* 31, 1457 (2011).

**Publisher's Note** Springer Nature remains neutral with regard to jurisdictional claims in published maps and institutional affiliations.